

# MAGNETIC PROPERTIES OF NITROGEN DOPING NIOBIUM SAMPLES\*

Z. Q. Yang, X. Y. Lu<sup>#</sup>, W. W. Tan, D. Y. Yang, Y. J. Yang, J. F. Zhao

State Key Laboratory of Nuclear Physics and Technology, Peking University, Beijing, China

## Abstract

Nitrogen doping study on Niobium samples used for the fabrication of superconducting radio frequency (SRF) cavities was carried out. The samples' surface treatments were attempted to replicate that of the cavities, which included heavy electropolishing (EP), nitrogen doping and the subsequent successive EP with different amounts of material removal. The magnetization curves of both doped and un-doped samples have been measured, from which the lower critical field  $H_{fp}$  (First Flux Penetration, ffp) and upper critical field  $H_{c2}$  was extracted. The thermodynamic critical field  $H_c$ , superheating field  $H_{sh}$  and superconducting parameters of samples with different treatments was calculated from the determined reversible magnetization curves.  $H_{sh}$  of doped samples is obviously smaller than that of un-doped samples, which may be a possible reason for the reduction of achievable accelerating gradient in SRF niobium cavities after nitrogen doping treatments.

## INTRODUCTION

Fundamental understanding of the nitrogen doping mechanism is being carried out extensively [1-5], but yet remains unclear. Two years after the discovery of nitrogen doping phenomenon, A. Romanenko [6] discovered that fast cooling down through  $T_c$  in both single cell and 9-cell nitrogen doping cavities helps to much more efficient flux expulsion and results in lower residual resistance. While this effect is not so obvious for un-doped cavities, especially for the cavities with standard preparation which consists of EP 120 $\mu$ m, 800 $^\circ$ C heat treatment for 3 hours, EP 20 $\mu$ m and 120 $^\circ$ C baking for 24-48 hours. A. Gurevich and G. Ciovati [7] studied the impact of vortex on the residual resistance of SRF niobium cavities. They predicted that the residual resistance has a high sensitivity to trapped flux. Dan Gonnella [8] studied the sensitivity of surface resistance to trapped magnetic flux on both doped and un-doped cavities. Dan Gonnella's experiments showed that nitrogen doping cavities have higher sensitivity of residual resistance to trapped flux. Vertical tests also showed that the sensitivity decreases with the EP removal and will be reduced gradually to the level of un-doped cavities after a certain amount of material removal, which is determined by the specific nitrogen doping condition.

For the nitrogen doping cavities, vertical tests [9-10] showed that the residual resistance has minimum value when the EP removal reaches an optimized value, where also corresponds to the largest quality factor. When the

EP removal is smaller or larger than the optimized value, the residual resistance becomes greater. So the variation of residual resistance with EP removal after nitrogen doping treatments is also an important aspect of the physical mechanism of nitrogen doping phenomenon. Limited to our experimental conditions, we tried to study the impact of nitrogen doping treatments on the residual resistance through experiments on Nb samples to seek the physical explanation of it.

As mentioned above, the diffused N may have an impact on the material's flux pinning behaviour and thereby affects the cavities' residual resistance. So it is necessary to study the magnetic properties of Nb samples before and after nitrogen doping treatment. Both doped and un-doped samples were electropolished with different amounts of material removal. Magnetic measurements on Nb samples were carried out with a SQUID magnetometer (Quantum Design MPMS-XL-7).

## EXPERIMENTAL PROCEDURE

To avoid heat generation, instead of wire electrodischarge machining (EDM), the niobium samples were manually processed. The niobium strips were polished smoothly on 180-grit sandpaper, 300-grit sandpaper and 1200-grit sandpaper. The samples' treatments were attempted to replicate that of the cavities. So the niobium strips were etched by EP (HF:H<sub>2</sub>SO<sub>4</sub>=1:9), with the material removal of about 150 $\mu$ m, to remove the mechanical damage layers and surface contaminations introduced during handling or exposing to the air.

### Nitrogen Doping Treatment

The nitrogen doping treatments and 800 $^\circ$ C heat treatments of the niobium samples used for the magnetic measurements can be seen in [11].

### Magnetization Measurement

The magnetization was measured by using a commercial SQUID magnetometer (Quantum Design MPMS-XL-7) at Peking University. The weight of experimental samples lies between 80-260mg. For the considerations of measurement range, the DC module was used with the measurement accuracy of  $1 \times 10^{-8}$  emu. Mounted in a sample holder, the sample was transported to the sample space together with a rigid sample rod during which the sample was cooled from room temperature at zero field (ZFC). The sample's motion length is 4cm. The magnetic field is homogeneous to 0.05% for this regime. The measuring range of DC applied field  $H_a$  lies between zero

\* Work supported by Major Research Plan of National Natural Science Foundation of China (91426303) and National Major Scientific Instrument and Equipment Development projects (2011YQ130018).

<sup>†</sup> Email address: xylyu@pku.edu.cn

Content from this work may be used under the terms of the CC BY 3.0 licence (© 2017). Any distribution of this work must maintain attribution to the author(s), title of the work, publisher, and DOI.

and 5000Oe, including an ascending branch and a descending branch. At each measuring point, the sample was driven through the detection coil and stopped at a number of positions over the specific scan length. The current induced by the magnetic moment of the sample would be detected by the superconducting detection coil, which can provide a highly accurate measurement of the sample's magnetic moment.

### Experimental Results

Two groups of samples were used in the magnetization measurements, labeled as "Test 1" and "Test 2", respectively. Magnetization curve of doped sample is shown in Figure 1 for reference, which is typical of type II superconductors.

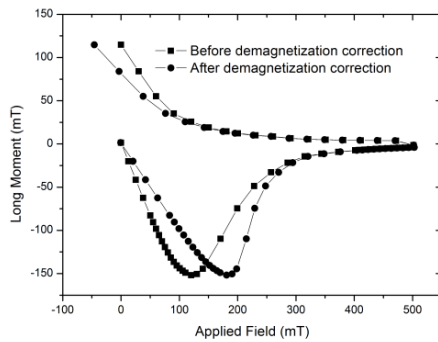


Figure 1: Magnetization curves of nitrogen doping sample before and after demagnetization correction.

$H_{ffp}$  (First Flux Penetration, ffp), which is  $H_{c1}$  for reversible magnetization curve, was determined by the field at which a deviation started from the linear magnetization  $M(H_a)$  in the Meissner state [12]. Deviation from the linear behavior means the disappearance of complete diamagnetism.

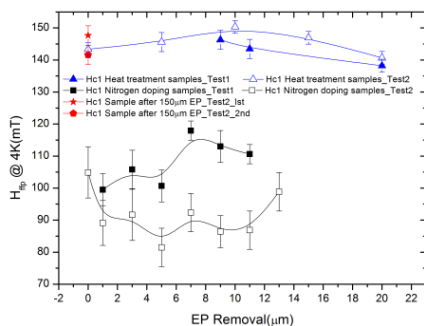


Figure 2:  $H_{ffp}$  of samples with different treatments.

$H_{c2}$  of all the samples is defined as the field at which the magnetization  $M(H_a)$  reaches zero.  $H_{c2}$  of all samples with different treatments is shown in Figure 3

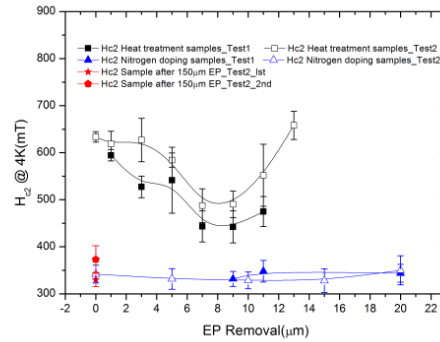


Figure 3:  $H_{c2}$  of samples with different treatments.

It can be seen in Fig. 2 that  $H_{ffp}$  of all doped samples is about 30% lower compared to the un-doped samples.  $H_{c2}$  of doped samples is significantly higher due to the diffused nitrogen.  $H_{c2}$  of doped samples in both Test 1 and Test 2 have the same change trend with the EP removal. The doped samples with EP removal 7-9 $\mu$ m have minimum  $H_{c2}$  in both Test 1 and Test 2. Both  $H_{ffp}$  and  $H_{c2}$  of doped samples failed to recover to the value of un-doped samples up to 13 $\mu$ m. This means the nitrogen doping effect of depth exceeds 13 $\mu$ m under our doping recipe.

### DETERMINATION OF REVERSIBLE MAGNETIZATION CURVE

A set of superconducting material parameters such as the Ginzburg-Landau parameter  $\kappa$ , the penetration depth  $\lambda$  and the coherence length  $\xi$  can be deduced from the relationship between  $H_{c2}$  and the thermodynamic critical field  $H_c$ . So  $H_c$  is the key of the analysis of magnetization measurements experimental data.

For niobium ( $RRR \approx 300$ ) used for SRF cavity fabrication, the magnetization curve shows significantly hysteresis. The reversible magnetization curve should be determined to assessment the superconducting parameters correctly.

The specific heat and magnetization measurements [13] showed that for  $H_c < H_a < H_{c2}$ , the thermodynamically deduced reversible magnetization curve is approximately equal to the average magnetization between increasing and decreasing fields:  $M_{rev} = (M_+ + M_-)/2$ , where  $M_+$  corresponds to the ascending branch and  $M_-$  to the descending branch. Torque magnetometry measurements by Willemin and co-workers [14] have shown the validity of the above procedure. Theoretical study of Kes [15] showed the reversible magnetization is indeed the average magnetization of the increasing and decreasing branches in first-order approximation. This will be the foundation of the determination of the reversible magnetization curve.

The complete reversible magnetization curve can be divided into four parts. That is the Meissner state part, the part near  $H_{ffp}$ , the part of intermediate field region (London region) and the part close to  $H_{c2}$  (Abrikosov region).

The completely determined reversible magnetization curve is shown in Fig. 4.

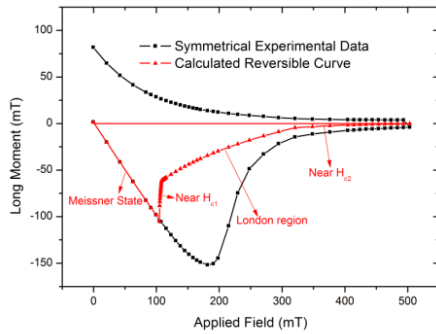


Figure 4: The calculated complete reversible magnetization curve that reflects the typical physical characteristics of ideal type II superconductor.

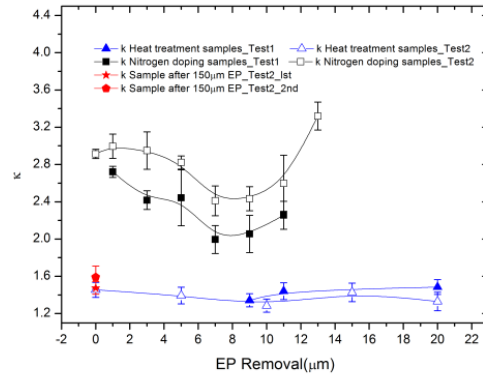


Figure 5: Ginzburg-Landau parameter  $\kappa$  of samples with different treatments.

Table 1: Thermodynamic Critical Field of Samples with Different Treatments in both Test 1 and Test 2

Test 1		Test 2	
Samples	$H_c$ at 0K/mT	Samples	$H_c$ at 0K/mT
N-D 1 $\mu$ m	190 $\pm$ 1	N-Doping 0 $\mu$ m	189 $\pm$ 12
N-D 3 $\mu$ m	189 $\pm$ 1	N-Doping 1 $\mu$ m	180 $\pm$ 1
N-D 5 $\mu$ m	192 $\pm$ 1	N-Doping 3 $\mu$ m	185 $\pm$ 4
N-D 7 $\mu$ m	193 $\pm$ 1	N-Doping 5 $\mu$ m	181 $\pm$ 1
N-D 9 $\mu$ m	187 $\pm$ 2	N-Doping 7 $\mu$ m	187 $\pm$ 9
N-D 11 $\mu$ m	183 $\pm$ 2	N-Doping 9 $\mu$ m	185 $\pm$ 1
H-T 9 $\mu$ m	214 $\pm$ 6	N-Doping 11 $\mu$ m	185 $\pm$ 8
H-T 11 $\mu$ m	210 $\pm$ 2	N-Doping 13 $\mu$ m	172 $\pm$ 1
H-T 20 $\mu$ m	201 $\pm$ 1	NoHTnoND 1 <sup>st</sup> *	195 $\pm$ 4
		NoHTnoND 2 <sup>nd</sup> *	204 $\pm$ 6
		HT-0 $\mu$ m	204 $\pm$ 6
		HT-5 $\mu$ m	207 $\pm$ 1
		HT-10 $\mu$ m	219 $\pm$ 1
		HT-15 $\mu$ m	200 $\pm$ 2
		HT-20 $\mu$ m	229 $\pm$ 2

\*Sample after EP 150 $\mu$ m without neither nitrogen doping treatment nor 800  $^\circ$ C heat treatment.

The calculated superconducting parameters such as  $\kappa$ ,  $\lambda$  and  $\xi$  can be seen in Figure 5, Figure 6 and Figure 7. The  $\kappa$  and  $\lambda$  of all doped samples is higher than that of un-doped samples, while the  $\xi$  of doped samples is lower. The diffused nitrogen can influence the niobium's  $\kappa$ ,  $\lambda$  and  $\xi$  value by changing the electron mean free path [16-17]. In both Test 1 and Test 2,  $\kappa$  and  $\lambda$  of doped samples have a minimum value between EP removals of 7  $\mu$ m to 9  $\mu$ m, which is also the location of the maximum value of  $\xi$ . This means the amount of trapped flux is least when the EP removal of doped samples is 7-9  $\mu$ m under our

experimental conditions. When the subsequent EP removal is less than 7  $\mu$ m, the amount of trapped flux decreases as the material removal increases. However, when the subsequent EP removal is more than 9  $\mu$ m, the amount of trapped flux increases with the sustained reduction of nitrogen impurity.

$H_c$  can be calculated from the reversible magnetization curve.  $H_c$  of samples with different treatments in both Test 1 and Test 2 is listed in Table 1. The thermodynamic critical field averaged over un-doped samples is 208 $\pm$ 10mT.  $H_c$  of doped samples is slightly smaller compared to the un-doped samples because of their lower  $H_{ffp}$ .

Content from this work may be used under the terms of the CC BY 3.0 licence (© 2017). Any distribution of this work must maintain attribution to the author(s), title of the work, publisher, and DOI.

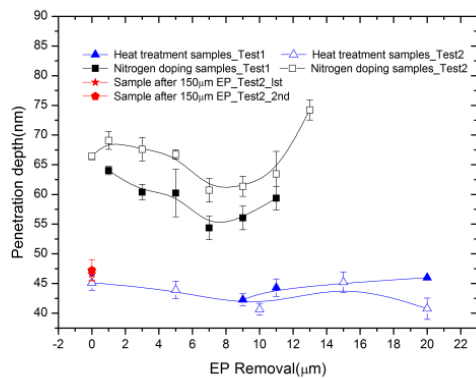


Figure 6: The penetration depth  $\lambda$  of samples with different treatments.

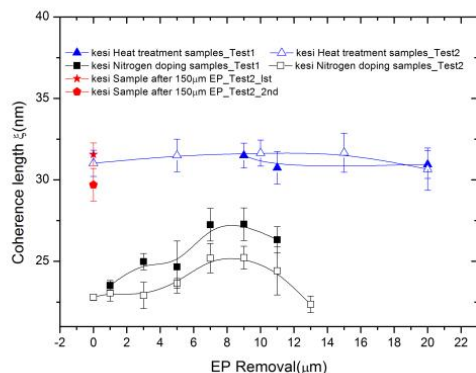


Figure 7: The coherence length  $\xi$  of samples with different treatments.

## SUPERHEATING FIELD

In the usual nanosecond timescale of an RF field, the RF critical field  $H_{rf, crit}$  is expected to be up to  $H_{sh}$ , which has been verified by high pulsed power measurements on both nitrogen doping cavity [18] and cavity with standard treatment [19]. Therefore,  $H_{sh}$  is the fundamental limit to the accelerating field for niobium cavity.

$H_{sh}$  can be estimated through the surface energy considerations. For microwave conditions, the  $H_{sh}$  can be calculated by [20]:

$$H_{sh} = \sqrt{2} \frac{H_c}{\sqrt{\lambda/\xi}} = \frac{\sqrt{2}}{\sqrt{\kappa}} H_c \quad (1)$$

$H_{sh}$  of samples with different treatments at 0K is shown in Figure 8.  $H_{sh}$  averaged over un-doped samples is  $227 \pm 6$  mT, which is in consistent with the estimated value of 240 mT in pure Nb.  $H_{sh}$  of doped samples is obviously smaller than that of un-doped samples.  $H_{sh}$  of doped samples in both Test1 and Test2 have the same change trend with the EP removal. The largest  $H_{sh}$  value of doped samples in Test1 and Test2 at 0K is  $177 \pm 6$  mT and  $161 \pm 6$  mT, respectively. This agrees well with the  $H_{sh}$  value of nitrogen doping cavity at 0K calculated from

material parameters using Ginzburg-Landau theory by Cornell University. The doped samples with EP removal 7-9  $\mu\text{m}$  have maximum  $H_{sh}$  in both Test 1 and Test 2. Measurements on nitrogen doping ingot niobium cavity, carried out by P. Dhakal and co-workers [9] from Jefferson Lab, have shown the breakdown field varied with successive material removal in the same way under their experimental condition.

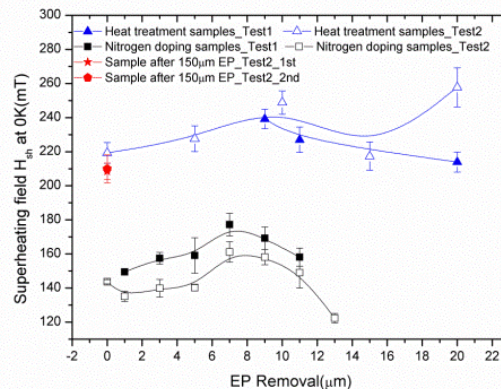


Figure 8:  $H_{sh}$  of samples with different treatments.

## CONCLUSION

DC magnetization measurements have been carried out to study the magnetic properties of Nb before and after nitrogen doping treatment.  $H_{fp}$  of all doped samples is about 30% lower compared to the un-doped samples.  $H_{c2}$  of doped samples is significantly larger than that of un-doped samples due to the decreased electron mean free path affected by diffused nitrogen.  $H_c$  and superconducting parameters such as  $\kappa$ ,  $\lambda$  and  $\xi$  were calculated from the determined reversible magnetization curves and they are consistent with each other. The dependence of  $H_{sh}$  on EP removal under our nitrogen doping condition is obtained.  $H_{sh}$  of doped samples is obviously smaller than that of un-doped samples, which may be a possible reason for the reduction of achievable  $E_{acc}$  in SRF niobium cavities after nitrogen doping treatments. For typical elliptical cavity geometry,  $H_p/E_{acc} = 4.2 \text{ mT/MV/m}$  leads to  $E_{acc} \sim 40 \text{ MV/m}$  as the fundamental limit to the nitrogen doping defect free Nb cavities under our experimental condition. Flux vortex may penetrate into the cavity at a field-enhanced defect, which may cause a smaller breakdown field.

## ACKNOWLEDGEMENT

The authors are grateful to L. Lin for his help in EP. The authors would also acknowledge Dr. Y. Zhang (Peking University) for the help in magnetization measurements. This work is supported by Major Research Plan of National Natural Science Foundation of China (91426303).



## REFERENCES

- [1] A. Grassellino, "High Q Development", in *Proceedings of IPAC'15*, Richmond, USA, 2015, talk MOYGB02.
- [2] A. Grassellino, "N doping: progress in development and understanding", in *Proceedings of SRF2015*, Whistler, Canada, MOBA06.
- [3] Y. Trenikhina et al., "Nanostructure of the penetration depth in Nb cavities: debunking the myths and new findings", in *Proceedings of SRF2015*, WEA1A05.
- [4] A. D. Palczewski, "Lessons learned from nitrogen doping at JLab", in *Proceedings of SRF2015*, MOBA07.
- [5] D. Gonnella, R. Eichhorn et al., "Improved N-doping protocols for SRF cavities" in *Proceedings of IPAC'16*, pp. 2323-2326
- [6] A. Romanenko, A. Grassellino, O. Melnychuk, and D. A. Sergatskov *J. Appl. Phys.* **115** 184903, 2014.
- [7] A. Gurevich and G. Ciovati 2013 *Phys. Rev. B* **87** 054502.
- [8] Dan Gonnella, John Kaufman, and Matthias Liepe, *J. Appl. Phys.* **119** 073904, 2016.
- [9] P. Dhakal, G. Ciovati et al., "Nitrogen doping study in ingot niobium cavities" *Proceedings of IPAC'15*, pp. 3506-3508.
- [10] G. Ciovati, D. Reschke and C. Reece, "WG3 Summary", *TTC Meeting*, Japan, 2014.
- [11] Z. Q. Yang et al., "TOF-SIMS study of nitrogen doping Niobium samples", in *Proceedings of SRF2015*, pp.169-173.
- [12] Roy S B et al., *Supercond. Sci. Technol.* **21** 065002, 2008.
- [13] R. Radebaugh and P. H. Keesom, *Phys. Rev.* **149**, 217-31, 1966.
- [14] M. Willemin, C. Rossel, J. Hofer, H. Keller, A. Erb and E. Walker, *Phys. Rev. B* **58**, pp.5940-5943, 1998
- [15] P. H. Kes, C. A. M. van der Klein and D. de Klerk, *J. Low Temp. Phys.* **10**, pp.759-779,1973.
- [16] A. B. Pippard, in *Proc. Roy. Soc. A* **216**, pp.547-568, 1953.
- [17] L. P. Gorkov, *J. Exp. Theor. Phys.* **36**, pp. 1364-1367, 1959.
- [18] J. T. Maniscalco, D. Gonnella et al., "Pulsed field limits in SRF cavities", in *Proceedings of IPAC'16*, pp.2341-2343.
- [19] T. Hays et al., in *Proceedings of the 7<sup>th</sup> Workshop on RF Superconductivity*, p.437, 1995.
- [20] K.Saito, "Critical field limitation of the niobium superconducting RF cavity", in *Proceedings of the 10<sup>th</sup> Workshop on RF Superconductivity*, Japan, 2001, pp.583-587.